RAPID COMMUNICATIONS

PHYSICAL REVIEW B VOLUME 46, NUMBER 11 15 SEPTEMBER 1992-I

Surface collective modes of non-neutral jellium

P. R. Pinsukanjana, E. G. Gwinn, John F. Dobson,* E. L. Yuh, and N. G. Asmar
Physics Department, University of California, Santa Barbara, California 93106

M. Sundaram and A. C. Gossard
Department of Electrical and Computer Engineering, University of California, Santa Barbara, California 93106

(Received 11 May 1992)

We report studies of the surface plasmon modes of a layer of electron gas that is embedded in a wider, effective positive background, provided by a parabolic $Al_xGa_{1-x}As$ well. Although conditions in the interior of the electron gas are nearly identical to those in a neutral jellium slab, the more abrupt electronic surfaces in the parabolic well produce a qualitatively different surface plasmon spectrum.

Electron gases in $Al_xGa_{1-x}As$ heterostructure wells provide experimental access to aspects of metal surface physics that are inaccessible in conventional metals. The principal advantages of the semiconductor system are as follows: the near-surface density profile of the electron gas can be tailored; the effective positive background can be chosen to be smooth; and the thickness of the electron gas is continuously variable from zero to a few Fermi wavelengths, so that the interesting crossover regime between two and three dimensions can be probed.

By their nature, the surface collective modes of an electron gas are sensitive to surface electronic structure.[1,2] We investigate surface plasmons on an electron gas that is embedded in a wider, effective positive background, provided by a parabolically graded, $Al_xGa_{1-x}As$ well.[3,4] The unusual nature of the surfaces in this non-neutral jellium produce a qualitatively different surface plasmon spectrum from that of a neutral jellium slab.[3] Although the optical, magneto-optical, and transport properties[5-12] of parabolic $Al_xGa_{1-x}As$ wells have been studied previously, this work presents an experimental study to address surface-related phenomena in such structures.

In $Al_xGa_{1-x}As$ heterostructure wells, varying the Al fraction, x, along the growth direction, z, varies the conduction-band edge, E_c, to realize a potential well for electrons. The well curvature $K=d^2E_c/dz^2$ determines an effective background charge density n_b, which by Poisson's equation is $n_b(z)=\epsilon K(z)/e^2$.[7] Remote donors, which lie in planes that are set back from either side of the well, provide conduction electrons. The nearly uniform, static fields of the planar sheets of ionized donors cancel in the well region between the donor planes, and should have little effect on the dynamic response of the electron gas.[13]

Neutral jellium is realized by adding a sheet density of electrons $N_e=n_bw_b$ to the potential well produced by a slab of positive charge with density n_b and width w_b. The electrostatic potential due to the positive slab is parabolic within the slab, and linear outside, as sketched by the dotted line in Fig. 1(a). The vertical, dashed lines show the slab boundaries, and the solid line shows a parabolic potential, for comparison. Non-neutral jellium is realized when $N_e<n_bw_b$: The layer of electron gas is then embedded in a wider positive background. In both the neutral and non-neutral cases, the electron gas forms a layer with density $n_e\cong n_b$, over a width $w_e\cong w_b$. The nominal width of the electron gas $w_e=N_e/n_b$. For the parabolic well studied here, the effective positive background extends at least four Thomas-Fermi screening lengths on either side of the electron layer, so the electron gas is well embedded.

In the interior of the electron gas, the parabolic well and neutral jellium are similar: The spacing of occupied single-electron levels are the same to within a fraction of a percent,[4] and the electron gas is nearly uniform. For temperatures below the Fermi temperature $T_F\sim 50$ K, the ratio of the characteristic potential and kinetic energies is similar to that in simple metals, although the electronic density in the semiconductor structure is ~ 6 orders of magnitude smaller. For the parabolic well studied here, $r_s=2.07$, where $r_s=r_0/a^*$, $(4\pi r_0^3/3)n_b=1$, and a^* is the Bohr radius in GaAs.

The conditions at the surfaces of the electron gas in a parabolic well are different from those at neutral jellium surfaces. Figure 1(b) plots the self-consistent potential $V(z)$ that results from adding a sheet density of electrons $N_e=n_bw_b$ to the confining potentials E_c shown in Fig. 1(a), for $n_b=2.75\times10^{16}$ cm^{-3} and $w_b=880$ Å. The extension of the positive background beyond the electron gas

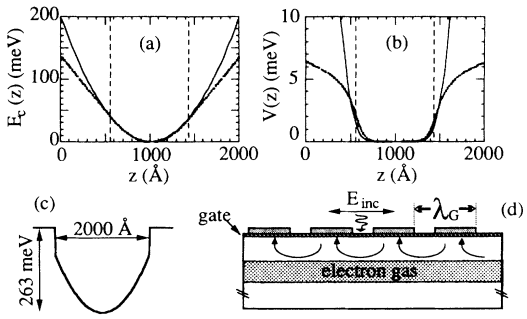

FIG. 1. (a) The dotted line shows electrostatic potential due to a uniform slab of positive charge with width $w_b=880$ Å and density $n_b=2.75\times10^{16}$ cm^{-3}. Dashed, vertical lines show boundaries of positive slab. The solid line shows parabolic potential for $n_b=2.75\times10^{16}$ cm^{-3}. (b) Total, self-consistent potential $V(z)$ for the wells in (a), for a sheet density of electrons $N_e=n_bw_b$. (c) Conduction-band edge $E_c(z)$ for PB31 (empty). Donor planes (not shown) are set back from the well edges by 200 Å. (d) Grating coupler; here $q_G=1.60\times10^4$ cm^{-1}. Vectors sketch fringing field.

in the parabolic well produces a steeper surface potential [solid line in Fig. 1(b)], and a corresponding steeper decay in the density at the surfaces of the electron gas. The different surface conditions shown in Fig. 1(b) have a marked effect on the surface plasmon spectrum.

Extensive investigations of collective electronic excitations in heterojunctions, square wells, and superlattices of square wells have been carried out.[14] All of these structures realize electron gases with density profiles that are sharply peaked in one or more sheetlike layers, and have different plasmon modes from the thick, nearly uniform layer of electron gas explored here.

We have studied a sample from a high-quality, molecular-beam epitaxy (MBE) grown parabolic well structure. Measurements of the Al flux during programmed growth sequences indicate that the well follows the design parabola closely, and extensive magnetotransport studies[12] show that the measured single-electron subband spacings agree with self-consistent calculations at the 3% level. Figure 1(c) sketches the conduction-band edge, E_c, for the empty well. The Al fraction, x, increases quadratically from $x=0$ at the well center to $x=0.2$ at the well edges at $z=2510$ Å and $z=4510$ Å, where z is measured from the sample surface. At the edges of the well, x steps up to 0.3. The design density[15] is $n_b=2.5\times10^{16}$ cm^{-3}, and corresponds to $\omega_p=50$ cm^{-1}.

We study the dependence of the surface plasmon spectrum on the continuously variable width, w_e, of the electron layer. A negative dc voltage bias V_G applied between a semitransparent gate that covers the sample surface, and an Ohmic contact to the electron gas, reduces w_e by moving the top edge of the electron gas away from the gate. We obtain the sheet density $N_e(V_G)$ and the width $w_e=N_e/n_b$ from the integral of $C(V_G)$, the measured capacitance between the gate and the electron gas. Magnetotransport measurements give $N_e(V_G)$ in agreement with that obtained from the capacitance. We also obtain d, the separation between the gate and the top surface of the electron gas, from the capacitance.[16]

To excite surface plasmons, we used a 3.92-μm period grating of Au bars to spatially modulate normally incident, far-infrared radiation.[17] Figure 1(d) sketches the fringing fields in the near field of the grating, which excite surface plasmons with wave vectors $q_\parallel=nq_G$, where $q_G=2\pi/\lambda_G$, λ_G is the grating period, and $n=1,2,\ldots$.[17] A 300-mK composite Si bolometer and a Bomem DAC.002 Fourier-transform spectrometer, set at nominal 0.5 cm^{-1} resolution, were used to collect far-infrared transmission data. The 2.90-mm diam sample was held at 1.5 K for all measurements.

Transmission spectra display both low- and high-frequency resonances, which arise from the coupling of charge fluctuations on opposite faces of the electron layer. Figure 2(a) shows the normalized transmission, $-\Delta T/T=\{T_0-T(w_e)\}/T_0$, where T_0 is the transmission through the empty well. The solid line corresponds to $w_e=880$ Å, and the dotted line to $w_e=580$ Å. As discussed below, we identify the resonances below 20 cm^{-1} and near 50 cm^{-1} as low and high frequency, coupled surface plasmons, ω_- and ω_+. Because we probe $q_\parallel\neq0$ only, we cannot measure $\omega_p^2=n_be^2/\epsilon m^*$ directly, but estimate that ω_p lies in the range 51–54 cm^{-1}, based on the observed range of ω_+ with w_e.

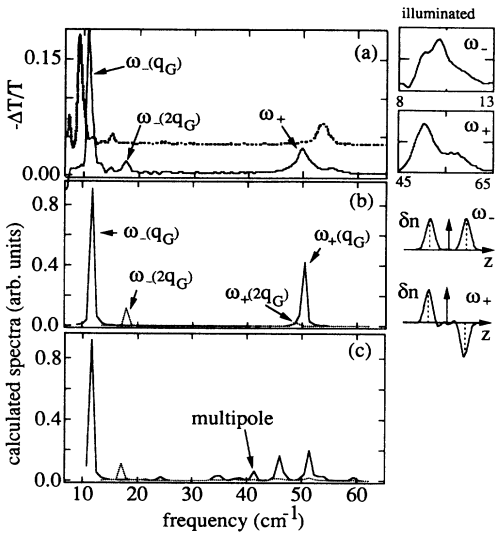

FIG. 2. (a) Solid and dotted lines show $-\Delta T/T$ prior to illumination for $w_e=880$ Å and $w_e=580$ Å (baseline offset), respectively. Insets to the right show illumination-induced splitting of the $\omega_-(q_G)$ resonance (top) and of the ω_+ resonance (bottom), for $w_e\sim500$ Å. (b) Calculated absorption spectrum for a parabolic well with $n_b=2.75\times10^{16}$ cm^{-3}, and $w_e=880$ Å for $q_\parallel=q_G=1.6\times10^4$ cm^{-1} (solid line) and for $q_\parallel=2q_G=3.2\times10^4$ cm^{-1} (dotted line). Insets to the right show the calculated, fluctuating surface plasmon charge $\delta n(z,\ q_\parallel=q_G)$ for the ω_- and ω_+ resonances. (c) Calculated absorption spectrum for a neutral jellium slab with $n_b=2.75\times10^{16}$ cm^{-3}, and $w_e=880$ Å.

For $q_\parallel=0$, the ω_+ resonance becomes the parabolic well sloshing resonance discussed in Ref. 10. Because the confining potential E_c is harmonic, the frequency of the sloshing mode is *independent* of w_e, and is equal to ω_p.[10] Resonances in parabolic wells at $\omega\cong\omega_p$ have been observed by other groups, and identified as the sloshing resonance.[5,6] Surface plasmons are a more general type of collective mode, which have frequencies that do depend on w_e.

Surface plasmon spectra for both neutral and non-neutral jellium layers have been calculated in the time-dependent, local-density approximation (TDLDA).[3] To simulate the grating coupler, an external potential $\delta\phi_{ext}=\exp(i[q_\parallel x-\omega t])\exp(q_\parallel z)$ was used, where $q_\parallel$ is the wave vector of the surface plasmon, and the electron gas lies at $z<0$. Surface plasmon resonances appear as peaks in $\mathrm{Im}[M(q_\parallel,\omega)]$, where

$$M(q_\parallel,\omega)=\left\{\int_{-\infty}^{\infty}dz\,e^{q_\parallel z}\delta n(z,q_\parallel,\omega)\right\},$$

and $\delta n(z,q_\parallel,\omega)$ is the induced charge density. The calculations assume $m^*/m_0=0.069$ and $\epsilon/\epsilon_0=13$; a constant $\mathrm{Im}(\omega)=1/\tau$, with $\omega_p\tau=300$; and include an image plane above the electron gas, which mimics the effects of the metallic gate and grating on the surface of the sample.

Figures 2(b) and 2(c) show the absorption spectrum $\omega\,\mathrm{Im}[M(q_\parallel,\omega)]$ for the parabolic well and for the neutral slab, respectively, for $n_b=2.75\times10^{16}$ cm^{-3} ($\omega_p=52.2$

cm^{-1}) and $w_e = 880$ Å. These parameters correspond to the experimental spectrum shown as a solid line in Fig. 2(a). The relative amplitudes of the calculated spectra for $q_\parallel = q_G$ (solid lines) and $q_\parallel = 2q_G$ (dashed lines) have been scaled to account for the coupling efficiency of the grating to the low-frequency resonance, in the limit that the electron gas becomes a two-dimensional sheet.[17] The unperturbed electron gas is calculated to occupy three subbands of the self-consistent potential $V(z)$ for $w_e = 880$ Å.

The form of the calculated parabolic well spectrum is simple: only two resonances appear, for fixed $q_\parallel$. As shown in the inset to the right of Fig. 2(b), the calculated, fluctuating charge of the surface plasmon, $\delta n(z,\omega_\pm)$, is localized near the surfaces of the electron layer. In contrast to the parabolic well, the calculated spectrum for the neutral jellium slab has a large number of weak resonances. The resonance near $0.8\omega_p$ (~ 42 cm^{-1}) has been identified[3] as the thin-layer analog of the multipole surface plasmon. This resonance becomes much stronger for lower electron densities and larger $q_\parallel$.

The qualitative differences between the spectra for the parabolic well and the neutral slab are due to the more abrupt electronic surfaces of the embedded electron gas. The multipole mode, for example, occurs only at electronic surfaces that are sufficiently diffuse.[18] This association of the simple spectrum for the parabolic well with its steep electronic surfaces is corraborated by calculated results for electron gases with surfaces that are steeper than in the parabolic well.[3] For example, if the central parabolic region occupied by the electron gas is bounded with quartic, rather than by quadratic, extensions, the absorption spectrum still shows only two resonances, with resonance frequencies ω_+ and ω_- that are both shifted slightly upwards from those of the parabolic well.[3]

The experimental transmission spectra for the parabolic well, shown in Fig. 2(a), are similar in form to the calculated spectra in Fig. 2(b). The two low-frequency resonances in the data can be identified from their dependence on w_e as $\omega_-(q_G)$, and $\omega_-(2q_G)$. The strong resonance near 50 cm^{-1} is the antisymmetric, coupled surface plasmon, ω_+. In the spectum for $w_e = 880$ Å, an additional, small peak appears above the main ω_+ resonance. This feature is not apparent in spectra for smaller w_e, and is discussed below. Because the damping processes that occur in the physical system are more complex than in the calculations, we do not expect agreement in the resonance strengths for the experimental and calculated spectra.

Figure 3(a) shows the dependence of the experimental ω_- on w_e. The vertical lines indicate subband occupation: Self-consistent calculations for $n_b = 2.75\times10^{16}$ cm^{-3} show that the second subband begins to fill at $w_e = 360$ Å, and the third subband at $w_e = 690$ Å. The dependence of the experimental ω_+ on w_e is shown in Fig. 3(b). No sharp features associated with subband filling are apparent in the data, for either resonance, in agreement with TDLDA calculations.

The resonance frequencies can also be estimated from a nonretarded, local optics model, in which the dielectric function of the electron gas is taken to be $\epsilon = \epsilon_2(1 - \omega_p^2/\omega^2)$ over its width w_e. Dielectrics with $\epsilon = \epsilon_1$ separate the electron gas from the gate, which is treated as a perfect conductor, and bound the back side of the electron gas. We obtain

$$\omega_\mp^2 = \frac{2\omega_p^2}{2+(\epsilon_1/\epsilon_2)(\coth(q_\parallel w_e)[1+\coth(q_\parallel d)] \pm \{\coth^2(q_\parallel w_e)[1+\coth(q_\parallel d)]^2 - 4\}^{1/2})} . \quad (1)$$

In the limit $d \to \infty$, for $\epsilon_1 = \epsilon_2$ Eq. (1) reduces to $\omega_\mp^2 = \frac{1}{2}\omega_p^2[1 \mp \exp(-q_\parallel w_e)]$, as is appropriate for a symmetric slab.[19] In the limit $w_e \to 0$, Eq. (1) becomes $\omega_+ = \omega_p$ and

$$\omega_-^2 = \frac{\omega_p^2(q_\parallel w_e)}{(\epsilon_1/\epsilon_2)[1+\coth(q_\parallel d)]} = \frac{e^2 q_\parallel N_e}{\epsilon_1 m^*[1+\coth(q_\parallel d)]} , \quad (2)$$

the well-known dispersion relation for the two-dimensional plasmon on an electron sheet of vanishing thickness.[17] For the range of $q_\parallel$ and w_e used in the experiment, the resonance frequencies calculated for the embedded electron gas in the TDLDA agree with Eq. (1), which becomes inaccurate for larger $q_\parallel$ and w_e than studied here. In contrast, for the neutral jellium slab, the local optics model fails qualitatively, even for small $q_\parallel w_e$.

Figure 3(a) shows ω_- from Eq. (1) (solid lines) and Eq. (2) (dashed lines), for $q_\parallel = q_G$ (lower curves), and for $q_\parallel = 2q_G$ (upper curves). Figure 3(b) shows $\omega_+(q_G)$ from Eq. (1). We have used $n_b = 2.75\times10^{16}$ cm^{-3}, $\epsilon_1 = 12.5\epsilon_0$ in the dielectric layers surrounding the electron gas, and $\epsilon_2 = 13.1\epsilon_0$ and $m^* = 0.069m_0$, which are the average values over the part of the well occupied by the electron gas for $w_e = 880$ Å. The observed frequencies deviate from the calculated values by as much as 6%. Possible origins for this discrepancy include variation in the curvature across the well, the abrupt step in the confining potential at its extreme edges [see Fig. 1(c)], and the spatial variation in m^* and ϵ.

Large-scale changes in the curvature of the part of the well occupied by the electron gas should produce extra resonances in the transmission spectra, which are not observed for $w_e \lesssim 880$ Å. Fluctuations in the curvature may be responsible for the larger linewidth of the ω_+ mode relative to the ω_- mode.

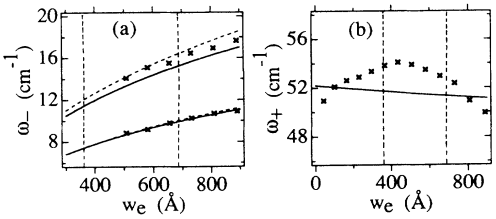

FIG. 3. (a) Dependence of ω_- on w_e. The solid lines show ω_- calculated from Eq. (1). The horizontal dashed lines show the 2D limit, Eq. (2). (b) Dependence of ω_+ on w_e. The solid line is $\omega_+(q_\parallel = q_G)$ from Eq. (1).

We estimate that the step in $E_c(z)$ at the edge of the parabolic well occurs $\sim$400 Å from the nearest surface of the electron gas, for $\omega_e = 880$ Å, if the density profile of the gas is idealized as rectangular. This is roughly 4 times the Thomas-Fermi screening length for an electron gas with $n_e = 2.75 \times 10^{16}$ cm^{-3}. The depth of the parabolic part of the well above the Fermi energy is at least $\sim$100 meV, or $\sim 16\hbar\omega_p$, for the data shown here. As w_e is increased, a weak resonance first appears above the main ω_+ peak in the spectrum for $w_e = 880$ Å [see Fig. 2(a)]. This may indicate the onset of the interaction of the tail of the electron density with the step at the edge of the confining potential. For larger w_e, transmission spectra show a series of several, substantially broadened resonances near 50 cm^{-1}.

The dependence of ϵ and m^* on the local Al fraction[20] produces $\sim$2% variation in the average of ϵm^* over the electron layer with w_e. Because the fluctuating charge of the surface plasmon is concentrated at the edges of the electron gas, the variation of ϵ and m^* at the surfaces may be more relevant. At the top surface on the electron gas, we estimate that m^* and ϵ vary by 9% and 2%, respectively, as the well is depleted.

The effects of static, spatial modulation of w_e on the experimental spectra are consistent with identification of the observed resonances as surface plasmons. Periodic modulation of w_e was produced by briefly illuminating the sample from its back side with an infrared LED. Because the gold grating has higher reflectivity than the Ti gate, w_e is weakly modulated, due to the persistent photoeffect.[21] Although a detailed analysis of the surface modes of a corrugated electron layer is complex,[22] qualitatively one expects that the modulation in w_e should open gaps in surface plasmon dispersion relations $\omega(q_\parallel)$, for $q_\parallel = m\pi/\lambda_G$, where $m = (\pm 1, \pm 2, \ldots)$.[23] Because the grating coupler excites plasmons with wave vectors $q_\parallel = 2n\pi/\lambda_G$, for $n = 1, 2, \ldots$, these gaps should split surface plasmon resonances, as has been observed for two-dimensional plasmons.[23] The insets in Fig. 2(a) show the effect of illumination on ω_+ and ω_-, for $w_e \sim 500$ Å. Both resonances split into two peaks, with a fractional splitting $\Delta\omega/\omega \cong 12\%$ and 9% for the ω_+ and ω_- resonances, respectively. If the ω_+ resonance were the parabolic well sloshing mode,[10] which has frequency independent of w_e, one would expect weak, static modulation of w_e to have little effect on the line shape.

We have shown that $Al_xGa_{1-x}As$ heterostructures can be used to realize quasi-three-dimensional metals with unusual surface properties, and that they provide a physical system in which to probe in detail the effects of surface conditions on surface electronic excitations. More detailed calculations are needed to understand the dependence of the observed resonance frequencies on w_e.

We acknowledge useful conversations with W. Kohn and S. J. Allen. This work was supported in part by NSF Grant No. DMR-9002491. Clean room use was supported in part by the NSF Science and Technology Center for Quantized Electronic Structures, Grant No. DMR88-10430.

---

*Present address: Division of Science and Technology, Griffith University, Nathan, Queensland 4111, Australia.

[1]P. J. Feibelman, Prog. Surf. Sci. **12**, 287 (1982).

[2]K. D. Tsuei, E. W. Plummer, and P. J. Feibelman, Phys. Rev. Lett. **63**, 2256 (1989); K. D. Tsuei *et al.*, *ibid.* **64**, 44 (1990).

[3]J. F. Dobson, Phys. Rev. B (to be published).

[4]N. G. Asmar and E. G. Gwinn, Phys. Rev. B **45**, 4752 (1992).

[5]K. Karrai *et al.*, Phys. Rev. B **39**, 1426 (1989); K. Karrai *et al.*, *ibid.* **40**, 12020 (1989).

[6]A. Wixforth *et al.*, Phys. Rev. B **43**, 1991 (1991).

[7]M. Sundaram *et al.*, Superlattices Microstruct. **4**, 683 (1988); E. G. Gwinn *et al.*, Phys. Rev. B **41**, 10700 (1990).

[8]T. Sajoto *et al.*, Phys. Rev. B **39**, 10464 (1989); T. Sajoto, J. Jo, and M. Shayegan, Appl. Phys. Lett. **55**, 1430 (1989).

[9]A. J. Rimberg and R. M. Westervelt, Phys. Rev. B **40**, 3970 (1989).

[10]L. Brey, N. F. Johnson, and B. I. Halperin, Phys. Rev. B **40**, 10647 (1989).

[11]M. P. Stopa and S. Das Sarma, Phys. Rev. B **40**, 10048 (1989).

[12]P. F. Hopkins *et al.*, Appl. Phys. Lett. **57**, 2823 (1990).

[13]Unequal charge transfer from the donor planes below and above the well can occur. If the donor sheets were perfectly uniform laterally, this would effectively add a linear term to the well in E_c, which would remain parabolic. Because the ionized donor sheets are not perfectly uniform, their fields will cause a small, random modulation of equipotential surfaces.

[14]For example, S. Das Sarma and A. Madhukar, Phys. Rev. B **23**, 805 (1981); D. Olego *et al.*, *ibid.* **25**, 7867 (1982); R. D. King-Smith and J. C. Inkson, *ibid.* **33**, 5489 (1986); T. Zettler, C. Peters, and J. P. Kotthaus, *ibid.* **39**, 3931 (1989); G. Fasol *et al.*, *ibid.* **39**, 12695 (1989); D. Richards, G. Fasol, and K. Ploog, Appl. Phys. Lett. **56**, 1649 (1990); and references in Ref. 17, below.

[15]To find n_b, we assume $\Delta E_c = 875x$(meV) and $\epsilon = 13\epsilon_0$. Because the orientation of the Al and Ga sources cause the curvature to vary laterally across the wafer, samples taken from different parts of the wafer will have somewhat different ω_p.

[16]C is well approximated by $C = \epsilon A/d$, for $\epsilon = 12.5\epsilon_0$, where A is the sample area: The average ϵ between the sample surface and the top edge of the well is $12.3\epsilon_0$, and the average ϵ from the sample surface to the bottom side of the well is $12.6\epsilon_0$ (Ref. 20).

[17]S. J. Allen, Jr., D. C. Tsui, and R. A. Logan, Phys. Rev. Lett. **38**, 980 (1977); T. N. Theis, Surf. Sci. **98**, 515 (1980); E. Batke, D. Heitmann, and C. W. Tu, Phys. Rev. B **34**, 6951 (1986).

[18]J. F. Dobson and G. H. Harris, J. Phys. C **21**, L729 (1988), and references therein.

[19]R. Ritchie, Phys. Rev. **106**, 874 (1957).

[20]S. Adachi, J. Appl. Phys. **58**, R1 (1985).

[21]R. Fletcher *et al.*, Phys. Rev. B **41**, 10649 (1990).

[22]H. Raether, *Surface Plasmons* (Springer-Verlag, Berlin, 1988).

[23]U. Mackens *et al.*, Phys. Rev. Lett. **53**, 1485 (1984).

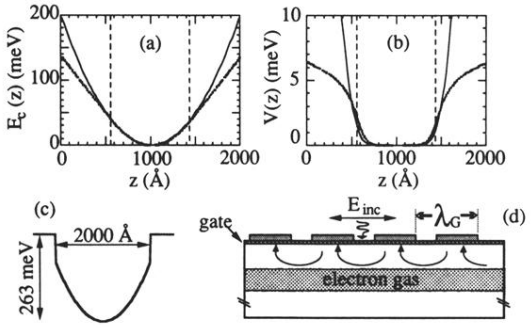

FIG. 1. (a) The dotted line shows electrostatic potential due to a uniform slab of positive charge with width $w_b = 880$ Å and density $n_b = 2.75 \times 10^{16}$ cm^{-3}. Dashed, vertical lines show boundaries of positive slab. The solid line shows parabolic potential for $n_b = 2.75 \times 10^{16}$ cm^{-3}. (b) Total, self-consistent potential $V(z)$ for the wells in (a), for a sheet density of electrons $N_e = n_b w_b$. (c) Conduction-band edge $E_c(z)$ for PB31 (empty). Donor planes (not shown) are set back from the well edges by 200 Å. (d) Grating coupler; here $q_G = 1.60 \times 10^4$ cm^{-1}. Vectors sketch fringing field.